A Review of Performance Characteristics of a Micro-strip Line

Gbayan Bundega Martins[1,a], Michael David [2,b], Michael Stephen Otor [2,c]

[1]Electrical and Electronics Engineering Department, University of Agriculture Markurdi, PMB 2373 Markurdi Benue State Nigeria

[2]Telecommunication Engineering Department, Federal University of Technology, Minna PMB 65 Minna Niger State, Nigeria

bundega@gmail.com [a], +2348069503793
mikeforheaven@futminna.edu.ng [b] michaelotor2004@gmail.com [c]

ABSTRACT

The basic characteristics of a micro-strip feed line for microwave patch element is studied and presented. The studied line is a straight rectangular shaped micro-strip line designed by Low Temperature Cofired Ceramics (LTCC) as a substrate and copper as the transmission line. A proposed method have been proposed for fabricating the LTCC tape, and the microstrip characteristics such as characteristic impedance which is found by mathematical equations to have a negative and non linear relationship with the width of the microstrip line. Also the transmission line losses are studied by interpreting the effect of the simulated geometry with mathematical model equation, the result for the study was interpreted and conclusions drawn. The effect of frequency on the microstrip was also studied by simulating the microstrip geometry. The result obtained gives a better understanding on general performance characteristic of a micro-strip line. The line is simulated using Comsol.

Keywords: *Transverse Electro-Magnetic (TEM), Radio frequency, micro-strip, electric field*

1 INTRODUCTION

A transmission line is the device used to guide radio frequency (RF) energy from one point to another (for example a coaxial cable). While an antenna is the structure associated with the region of transition from a guided wave to a free space wave, radiating RF energy (Authors, 2013). IEEE defines antenna as a means for radiating or receiving radio waves (Victor Bernard, 2013).
The demand for transmission lines in RF and microwave circuit has become inevitable in virtually all spheres of signal transfer and manufacture of RF and microwave components. Among the transmission lines the planer transmission line namely micro strip line and co-planner lines are the most useful in modern electronics. Micro-strip line is the most widely used type of planner transmission line RF and microwave integrated circuits (Nguyen, 2001) (Amit Kumar, 2013) (Chang, 2004). The popularity of this transmission line comes from its ease of fabrication, miniaturization and integration with microwave devices (Nguyen, 2001) (Amit Kumar, 2013) (Chang, 2004) (Pozar, 2012). Its geometry consist of a substrate which is a dielectric material sandwiched between two conductors, the strip line and the ground plan which for this research will be assumed to have zero thickness as shown in Figure 1. The substrate used is Low Temperature Co-fired Ceramic (LTCC) and copper is used as the strip line.
The dielectric cover only part of the conduction strip during transmission therefore, not all the field is contained within the substrate, some of it is contained in the air region above the substrate. Hence the surface wave produced by this geometry (microstrip line) is a hyridized coupling of Transverse Electric (TE) and Transverse Magnetic (TM) wave and other boundary conditions imposed by air and dielectric substrate interface to form an impure Transverse Electro-Magnetic (TEM) wave unlike coaxial line and strip line that are pure TEM. The wave found in this line is called quasi-TEM. The quantity of TEM in the substrate is a function of relative permittivity of the substrate and can be determined by $\frac{c}{\sqrt{\varepsilon_r}}$. Where c is the speed of light and ε_r is relative permittivity of the substrate.
The effective dielectric constant, characteristic impedance and attenuation of the quasi-static TEM and also the current distribution on the strip conductor is not uniform at different frequencies, this non uniformity particularly in current could lead to parasitic reactances and higher order modes, (Pozar, 2012) and other changes in line parameter could lead to phase delay, signal dispersion and distortion in the input signal
In this paper a micro-strip transmission line is modelled and simulated to find the effects of the geometry and relative permittivity on the characteristic impedance. The losses in the line is also investigated using Rodger calculator. Investigation of the loses is achieved by imputing the dimensions of the micro-strip and material properties of the LTCC into the calculator. The dimensions and the material properties in the Roger calculator is also imputed into Comsol multi-physics software and simulated.

1.1 PROPOSED METHOD OF FABRICATION

The iterative process require for the LTCC fabrication depend on the manufacture of the tape. Common manufacturers of the green tape are Dupont, Electro-Science Lab, EMCA Remex and Ferro (P. E. Garrou,

1998) (Golonka, 2006) (Gbayan, 2014) (DuPont™, 2017). Unfired LTCC tapes are purchased from the manufacturer in various dimensions. After it is purchased the tape is slit into desired dimensions with tolerance consideration. The tolerance differ for different manufacturers. For DuPont the tolerance range is ± 4 . For this proposed fabrication the tape is cut to $3120\mu m \times 260\mu m$ to allow for shrinkage during heating. The tape is then baked at $120°C$ for $30min$ to ease the stress in the tape and allow for appropriate shrinkage. The tape is then fabricated mechanically by cutting, drilling and thinning the tape using a laser machining. Other laser process beside the laser machine like punching, chemical etching and mechanical milling can also be used to perform this process, but the laser machining is proposed here because of its ability to support complex geometry fabrication of very small dimensions and it require no contact with the tape thus avoiding stress in the tape and supporting high accuracy, density and volume process possibility. After the laser machining process the tape is then screen printed with a conductive paste for example copper using a stencil. The screen printed LTCC sheet is then sintered or co-fired.

2 MICRO-STRIP MODEL

Figure 1: Microstrip line (Pozar, 2012)

A straight microstrip with copper width (w), $250\mu m$, and thickness (t), $95\mu m$, and permittivity (ε) is mounted on an LTCC with permittivity (ε). Copper was chosen in the design because of its relative availability, low market value and high melting point compared to the LTCC substrate, while LTCC is chosen because of low effective microwave circuit package, its ability to be fabricated in 3-D, its support for monolithic technology, increased design flexibility by supporting integration of active and passive devices and its low loss characteristics of the dielectric. Some electrical properties of LTCC are presented in Table 1 (Ramash Garg, 2013). More properties on LTCC can be read in (DuPont™, 2017)

Table 1: LTCC Electrical Properties

Electrical properties	green Tape 951
Dielectric constant (10GHz)	7.8 ∓ 0.2
Loss tangent (10GHz)	0.0140
Breakdown voltage(kV/25um)	>=1000

3 MATHEMATICAL AND GEOMETRY MODEL

The effective permittivity ε_{eff} and characteristic impedance Z_0 of the substrate assuming the entire microstrip is covered by a single dielectric constant can be found for different geometries of the conductor from equation 1-4.

The designed geometry has conductor a length (l), $3000\mu m$,width (w), $250\mu m$ to height (h),$95\mu m$.

For a conductor with $\frac{w}{h} \leq 1$ and , $\frac{w}{h} > 1$ the effective permittivity (ε_{eff}) as given by the following authors (Victor Bernard, 2013) (Chang, 2004) (Jai-Sheng Hong, 2001) (Antti V Raisanen, 2003) (Misra, 2001) (Ali Elrashidi, 2012) and (Rajat Arora, 2013) are:

For $\frac{w}{h} \leq 1$

$$\varepsilon_{eff} = \frac{\varepsilon_r+1}{2} + \frac{\varepsilon_r-1}{2}\left[\left(1+\frac{12h}{w}\right)^{-\frac{1}{2}} + 0.04\left(1-\frac{w}{h}\right)^2\right] \quad (1)$$

Where ε_r is the relative permittivity.
The characteristic impedance Z_0 for this geometry is calculated as

$$Z_0 = 60\left(\varepsilon_{eff}\right)^{-\frac{1}{2}} \ln\left(\frac{8h}{w} + \frac{0.25w}{h}\right)\Omega \quad (2)$$

And for width to height ratio greater than unity $\left(\frac{w}{h} > 1\right)$ ε_{eff} for the same conditions as equation 1 becomes

$$\varepsilon_{eff} = \frac{\varepsilon_r+1}{2} + \frac{\varepsilon_r-1}{2}\left(1+\frac{12h}{w}\right)^{-\frac{1}{2}} \quad (3)$$

Characteristic impedance Z_0 is expressed as:

$$Z_0 = \frac{\left[120\pi\left(\varepsilon_{eff}\right)^{-\frac{1}{2}}\right]}{\left(\frac{W}{h}\right)+1.393+0.667\ln\left(1.444+\frac{W}{h}\right)}\Omega \quad (4)$$

It will be observed from equation (1-4) that the width, height, and relative permittivity, are primary parameters that determine the properties of a micro-strip line. And the effect of this properties is determined by the ratio of this properties of the transmission line.
The effective permittivity of the micro-strip is determined by the ε_r of two materials, air with $\varepsilon_r \approx 1$ and another material with $\varepsilon_r > 1$. Therefore the effective permittivity(ε_{eff}) of the entire line will satisfy a relationship $\varepsilon_r > \varepsilon_{eff} > 1$.
And ε_{eff} determines the phase delay of the line section. The phase delay is determined through the relationship from the relationship between wave number or

propagation constant or phase constant k_0, line length l, and effective dielectric constant ε_e (Pozar, 2012) as

$$\emptyset_0 = \sqrt{\varepsilon_{eff}}\, k_0 l \quad (5)$$

4 RESULTS AND DISCUSSION

4.1 Relationship between Characteristic Impedance and Geometry (W/H) Using Approximate Formula

Figure 2 shows the relationship between characteristic impedance and geometry. This was obtained by varying the width of the conductor line and fixed thickness of the co-fired ceramics at 95microns.

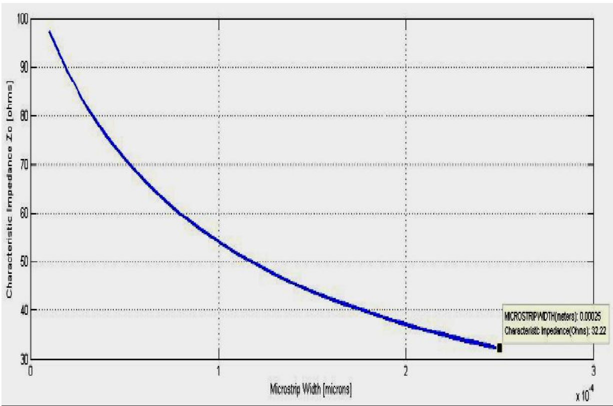

Figure 2: Effect of Conductor Width on Characteristic Impedance

ε_{eff} of the wave is related to phase velocity of the wave by $v_p = \frac{\omega}{\beta} = \frac{c}{\sqrt{\varepsilon_{eff}}}$ and propagation constant by $\beta = \frac{2\pi}{\lambda_g} = k_0\sqrt{\varepsilon_{eff}}$ and wavelength of the guided wave in the line is given by

$$\lambda_g = \frac{\lambda_0}{\sqrt{\varepsilon_{eff}}}. \quad (6)$$

4.2 Loss Model

A micro-strip line is design to transmit with very low, possibly zero radiation losses. However, since the conductor is partly exposed to free space, radiation losses become an important problem. The rate of radiation loss of a conductor is dependent on either the thickness of the circuit or the dielectric constant of the circuit.

A thick circuit will have higher radiation losses than a thin circuit. While a large dielectric constant will have higher radiation loss than a smaller dielectric constant circuit.

4.3 Conduction Loss

These are losses caused by electrical resistance (R_s) between the strip conducting and the ground. This loss is given by

$$\alpha_c = \frac{\sqrt{\frac{\omega\mu_0}{2\sigma}}}{Z_0 W} \text{ Np/m} \quad (7)$$

Where σ is conductivity of the material used as microstrip line and $\mu_0 = 4\pi \times 10^{-7}$ is the permeability of free space. From Figure 3 it can be seen that the micro-strip has an initial sharp increase in conductor loss before 5GHz and then it increase steadily at higher frequencies.

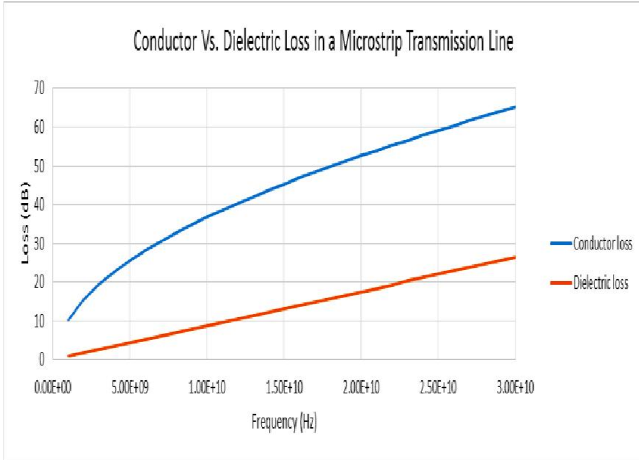

Figure 3: Comparison between Dielectric Losses and Conductive Losses Using Rodgers Calculator

4.4 Dielectric Loss

This is a loss caused by dissipation of the transmitted energy. It is given by

$$\alpha_d = \frac{k_0\varepsilon_r(\varepsilon_{eff}-1)\tan\delta}{2(\varepsilon_r-1)\sqrt{\varepsilon_e}} \quad (8)$$

Where $\tan\delta$ is the loss tangent of the dielectric which is expressed as a complex plane as resistive and reactive components, $k_0 = \frac{2\pi f}{c}$ is the free space wave number measured in rad/m and $\frac{(\varepsilon_{eff}-1)}{(\varepsilon_r-1)}$ is the microstrip field line filling factor. For most microstrip lines the dielectric losses is usually smaller than the conductor loss. However, dielectric loss of a silicon substrate can be of same order or larger than conductor losses.

Total losses = dielectric + conductor + radiation

From Figure 3 it is observed that the micro-strip has a steady frequency increase from almost zero dB at all frequencies under the study

5 SIMULATION

The micro-strip geometry was built using Radio Frequency physics using Electromagnetic Frequency Domain COMSOL in the 3D model wizard. The global parameter definition and the boundary conditions for the different domains namely, the air and the micro-strip domain was set. The designed geometry was then messed into discretised finite elements and a study was made for the different frequencies to study their response using parametric sweep. An image snapshot of the simulation is shown Figure 4 below.

5.1 DIAGRAM OF SIMULATED BLOCK

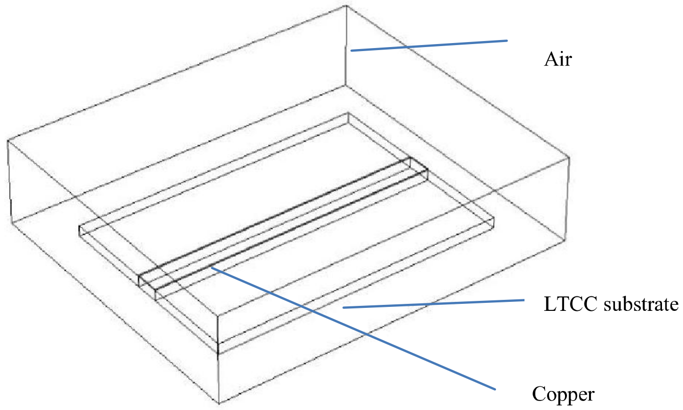

Figure 4: Un-simulated geometry of micro-strip transmission line with substrate length =3000microns, thickness=95microns and width =2095microns and conductor length =3000microns, thickness =95microns and width =250microns.

.

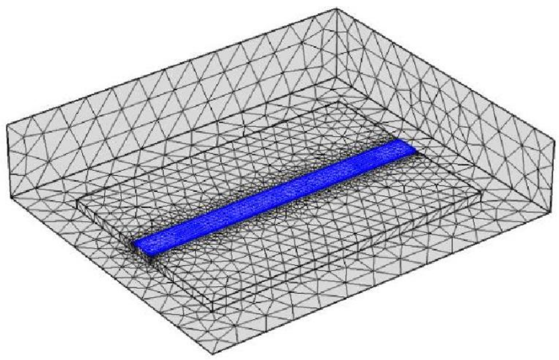

Figure 5: Meshed micro-strip line of the transmission line with three hidden faces to get a clear view of the substrate and the strip line.

5.2 SIMULATION RESULTS

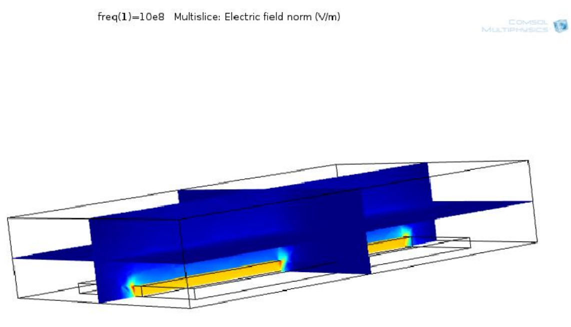

Figure 6: Electric field of Simulated microstrip design. Showing the electric field distribution in the copper at 1GHz

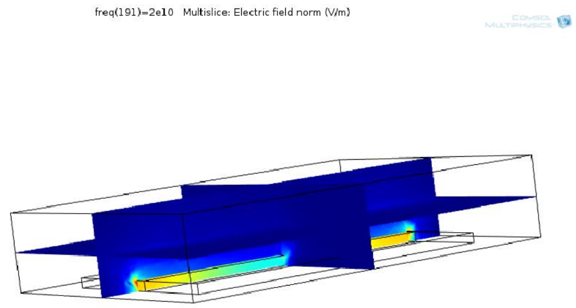

Figure 7: Electric field of Simulated microstrip design. Showing the electric field distribution in the copper at 20GHz

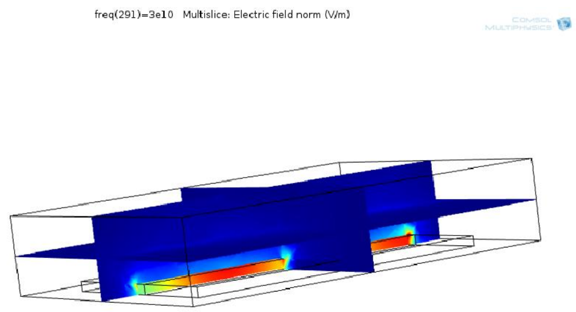

Figure 8: Electric field of Simulated microstrip design. Showing the electric field distribution in the copper at 30GHz

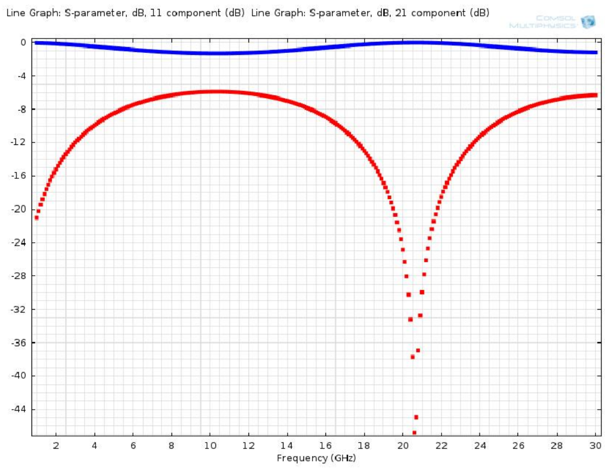

Figure 9: S-Paramters, showing the signal performance over different frequencies.

The simulation result show different responses of the transmission line at various frequencies as can be seen from the different colours shown by the electric field radiation from Figure 6-8. In Figure 6 it will be seen that the microstrip line has an almost even distribution of yellow radiation along the strip line. This radiation distribution become less even in Figure 7 and Figure 8 has the most uneven distribution of electric field along the transmission line. Also Figure 8 has the brightest distribution of the electric field. The electric field effect of the transmission line is as a result of skin effect of the frequency on the line. Which causes the electric field to flow more on the surface of the transmission line, thus making its effect more obvious. Figure 9 shows the worse frequency attenuation of -47dB at 20.5GHz for the simulated frequencies

6 CONCLUSION

From the result obtained in the paper it can be concluded that the level of signal attenuation in a micro-strip transmission line could have a linear and non linear relationship depending on the frequency of transmission frequency, and this can be seen from the simulation results and the mathematical equation presented. At higher frequency, the amount of attenuation increase and vice-versa. The amount of conduction loss is also larger than the dielectric loss. The design geometry can also be simulated using commercial software. It was also observed that the effect of electric field on the simulated geometry changes and show unevenness in distribution over the copper strip at different frequencies.

7 REFERENCES

Ali Elrashidi, K. E. (2012). Input impedance, VSWR and return loss of a conformal microstrip printed antenna for TM01 Model using two different substrates. *International journal of Networks and Communications*, 13-19.

Amit Kumar, J. K. (2013). Performance Analysis of Different Feeding Techniques. *International Jornal of Emerging Technology and Advanced Engineering*, 884-890.

Antti V Raisanen, A. L. (2003). *Radio Engineering for Wireless Communication and Sensor Applications.* Artech house.

Authors, T. W. (2013). Antenna/ Transmission Lines. In W. Authors, *Wireless Networking in the Developing World, A practical guide to planning and building low-cost telecommunication infrastructure* (pp. pp 54-82). Creative Common Attribution-Sharelike 3.0 licences. Retrieved from http://wndw.net: http://wndw.net

Chang, K. (2004). *RF and Microwave Wireless System.* John Wiley and Sons, Inc.

DuPont™. (2017, January 27). *Low temperature co-fired ceramic system*. Retrieved from Du Pont: http://www.dupont.com/

Gbayan, B. M. (2014). *Rapid Prototyping Of Micro Electro Mechanical System (Mems) Devices By Low Temperature Co-Fired Ceramics (Ltcc).* Leeds.

Golonka, L. (2006). Technology and applications of Low Temperature Cofired Ceramic (LTCC) based sensors and microsystems. *Bulletin of the Polish Academy of Sciences Technical Sciences*, pp. 221-231.

Jai-Sheng Hong, M. L. (2001). *Microstrip Filter for RF/Microwave Applications.* John Wiley & Sons, Inc.

Misra, D. K. (2001). *Radio-Frequency and Microwave communication circuits analysis and design.* John Wiley & Sons, Inc.

Nguyen, C. (2001). *Analysis methods for RF, microwave and millimetre wave planer transmission line structure.* John Wiley & Sons, Inc.

P. E. Garrou, I. T. (1998). *Multichip module technology Handbook.* New York, London: McGraw-Hill.

Pozar, D. M. (2012). *Microwave Engineering.* John Wiley and Sons, Inc.

Rajat Arora, A. K. (2013). Finite element modelling and design of rectangular patch antenna with different feeding techniques. *Scientific journal of Open journal of Antenna and propagation*, 11-17.

Ramash Garg, I. B. (2013). *Microstrip Lines and Slot lines.* Artech house.

Victor Bernard, J. P. (2013). Microstrip Antenna Design Using Transmission Line Model. *International*

Journal of Emerging Technology and Advanced Engineering, 410-415.

8 APPENDIX

For $\frac{w}{d} < 2$

$$\frac{w}{d} = \frac{8e^{\frac{Z_0}{60}\sqrt{\frac{\varepsilon r+1}{2}}+\frac{\varepsilon r-1}{\varepsilon r+1}\left(0.23+\frac{0.11}{\varepsilon r}\right)}}{e^{2\left(\frac{Z_0}{60}\sqrt{\frac{\varepsilon r+1}{2}}+\frac{\varepsilon r-1}{\varepsilon r+1}\left(0.23+\frac{0.11}{\varepsilon r}\right)\right)}-2} \quad (9)$$

And for $\frac{w}{d} > 2$

$$\frac{w}{d} = \frac{2}{\pi}\left[\frac{377\pi}{2Z_0\sqrt{\varepsilon_r}} - 1 - \ln\left(2\left(\frac{377\pi}{2Z_0\sqrt{\varepsilon_r}}\right) - 1\right) + \frac{\varepsilon_r - 1}{2\varepsilon_r}\left\{\ln\left(\frac{377\pi}{2Z_0\sqrt{\varepsilon_r}} - 1\right) + 0.39 - \frac{0.61}{\varepsilon_r}\right\}\right] \quad (10)$$